Auxiliary Resonant Scanner to Increase the Scanning Capability for Coarse Integral Holographic Displays

Jhen-Si Chen[1], Quinn Smithwick[2], Jin Li[1], Daping Chu[1,*]

[1]*Centre for Photonic Devices and Sensors, University of Cambridge, 9 JJ Thomson Avenue, Cambridge CB3 0FA, UK*

[2]*Disney Research, Glendale, CA 91201-5020, USA*
*Corresponding author: dcp31@cam.ac.uk

This paper proposes a scanned holographic display system which takes the advantage of a high-speed resonant scanner to augment a galvanometer and hence improves the opto-mechanical information distribution capabilities, thereby potentially achieves the increased image size and the enlarged viewing angles.

OCIS Codes: 090.1995, 070.7345, 100.6890.
doi:10.3788/COLXXXXXX.XXXXXX.

With the ability to provide all the necessary visual depth cues [1, 2], 3D holographic displays have the potential to be the ultimate 3D images displays, attracting research efforts in the past decades [3, 4]. To deliver 3D images with depth cues, the system needs to provide enough information, with sufficient bandwidth both optically and digitally, regardless of the optical system.

An example is illustrative of the requirements of a representative system. A 1,000 ×1,000 pixel phase-only hologram with a pixel pitch of 10 μm can project 3D images of 10 mm × 10 mm extent with 3.6° × 3.6° viewing angle, assuming the wavelength is 633 nm (red light). The image size and the viewing angle are exchangeable while their product is a constant because of the Lagrange Invariant [5]. Having 50 mm × 50 mm × 10° × 10° × 3 (R/G/B) × 30 frames/sec requires more than 17 Gpixels/sec. Note that shorter wavelengths, such as 520nm (green) and 450nm (blue), have smaller viewing angles than the red light, so they require more bandwidths for the same visual range. Considering the necessary bits per pixel, which is expected to be 8 bits to meet the commercial graphic standard, the overall bandwidth will be more than 100 Gbits/sec. Furthermore, the size and the viewing angle of this example are smaller than what general applications need. It is likely that 1 Tbits/sec or more is necessary. Therefore, there is a need to develop high bandwidth spatial light modulators (SLM) to meet this requirement before the practical 3D holographic display is feasible.

When we consider high-bandwidth devices, they can be categorized into two types: a high space bandwidth product (SBP) with a typical video rate frame-rate and a typical video-resolution SBP with a high frame-rate. In the former case, for example, if the SLM can be made up to 100,000 × 100,000 pixels with 60 frames/sec, it can directly be used to support a holographic image of a large image size and a wide viewing angle. Unfortunately, this is not feasible due to practical issues, such as the pixel uniformity and the control of electronic signaling. Digital micro-mirror device (DMD) is a good example for the latter case. To fully utilize its bandwidth for holographic

applications, there is a need to distribute frames efficiently so information contributes to visual imagery rather than being wasted. For example, a DMD supporting a 1,024 ×768 frame resolution with 22,727 frames/sec provides 17 Gpixels/sec. Distributing this information for holographic 3D images requires careful system integration and appropriate hologram computation. Our previous works in coarse integral holography (CIH) [6] and layer-based algorithm [7] were trying to deal with these difficulties. Principles of CIH will be briefly introduced shortly. However, our previous implementation of the scanned CIH system is limited by the capability of the physical scanner. Therefore, this paper proposes an approach to incorporate an auxiliary resonant scanner to expand the information distribution capability of the scanned CIH system. It will be introduced later.

Coarse integral imaging [8, 9] is a technique to angularly tile 2D images to generate multiple 2D views. CIH takes advantage of this concept and replaces the 2D images sources with holograms carrying 3D images information [6]. CIH further takes advantages of holograms to integrate the phase profile of the lenslet of the lens-array used in coarse integral imaging into hologram calculations, so that the overall system is simpler and easier to implement. Fig.1 illustrates the scanned CIH concept. The previous prototype demonstrated a full-color, full-parallax, 23.33-fps holographic video of a modest horizontal and small vertical viewing angle; although it only uses around a half of the bandwidth on the VGA DMD with the maximum 22,727 frame/sec. Systems using scanners to distribute information from binary SLM(s) can also be found in [10,11].

The scanned CIH architecture couldn't use the full bandwidth of the DMD because of the limited scanning speed of the galvanometer. One possible approach to improve is to replace the mirror substrate (aluminum on the current scanner) with a material with a higher strength-to-weight ratio, such as Beryllium, so that the mirror can sustain a higher scanning speed without being

broken. However, the mirror substrate with the specific material is significantly more expensive.
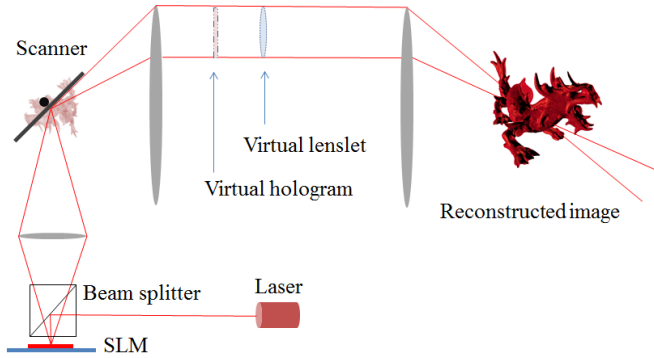

Figure 1. Illustration of the CIH system.

To more clearly explain the limitation, we explain the scanning mechanism and define the scanning capability. CIH angularly tiles the holographic images, and each sub-hologram provides a small viewing angle of the target 3D images/scene (horizontally and vertically), say $\Delta\theta x \times \Delta\theta y$. Adjacent sub-holograms should be projected at an adjacent view $\Delta\theta x$ away from the previous view. The CIH scanning pattern is designed as shown in the left part of Fig.2, so each frame has a horizontal viewing angle of $m \cdot \Delta\theta x$ and vertical viewing angle of $n \cdot \Delta\theta y$, where m is the number of views in each scanline and n is the number of scanlines. Note that the scanning is continuous, so the image is dragged along the scanning angularly before the sub-hologram is updated on the DMD. This can cause blurring if continuous laser is in use, and its effect can be minimized if a pulsed laser is in use.

The overall scanning route is based on a boustrophedon pattern to minimize the flyback issue and maximize the efficiency. The width of the horizontal scan is proportional to the overall horizontal viewing angle, while the number of horizontal scanlines multiplied by the sub-hologram view angle $\Delta\theta y$ represents the overall vertical viewing angle. It is clear that it is best to scan horizontally as wide as possible and also to provide as many scanlines as possible. However, the horizontal scan angle and the number of available scanlines are mainly limited by the galvanometer performance.

The first axis of the galvonameter in previous CIH system can be driven at 70 Hz with 24° optical scanning angle. Each forward-backward movement can be divided into two scanlines when the second axis of the galvanometer synchronously switches, resulting a total of 140 scanlines/sec. For the DMD in use, the horizontal scan width can at most accommodate 30 sub-holograms without overlapping. This is calculated based on the frame width and the viewing angle produced with the blue wavelength (450 nm). With a fixed frame rate of DMD, it means unavoidably there are overlapping for green and red wavelengths, so red and green views are chopped to match the blue field of view. Overall, 30 sub-views × 3 colors × 140 lines = 12,600 sub-holograms, which is around 55% of the DMD's 22,727 frames/sec

frame rate. Note that details and specifications about our previous work, dynamic CIH system, can be found in [6].

Here we define the scanning capability for comparison later and use the first axis of the galvanometer as an example. The scanner axis has a mirror supporting an aperture of 24.7 mm × 24.7 mm. Each 1,024 × 768 pixels hologram projected onto the mirror represents a $\Delta\theta x \times \Delta\theta y = 0.8° \times 1.06°$ viewing angle for the blue wavelength (nm). This confirms the number of 30 sub-holograms in the last paragraph: 24°/scanline ÷ 0.8°/sub-hologram = 30 sub-holograms/line

We can define scanning capability, C, to be C = horizontal_scan_range × $\Delta\theta_{vertical}$ × scan_line/second × area. For our previous system, C~3.2 ×10⁶ mm² ·deg² ·lines/sec (= 24°×1.06°×140 line/sec × 30mm × 30mm). Note that in our previous work (the galvanometer set-up), the scanning direction is x axis, and the whole supported viewing angle is the horizontal scanning range in x axis and $\Delta\theta_y$ in y axis for each scan line. We use this to evaluate the scanning capability.

If the mirror area is reduced, the scanning capability can be increased when the scanning speed can be increased disproportionately faster to compensate the size reduction. However, this is not ideal because it means a smaller image size. In our system, we have a minimum image size requirement to meet.
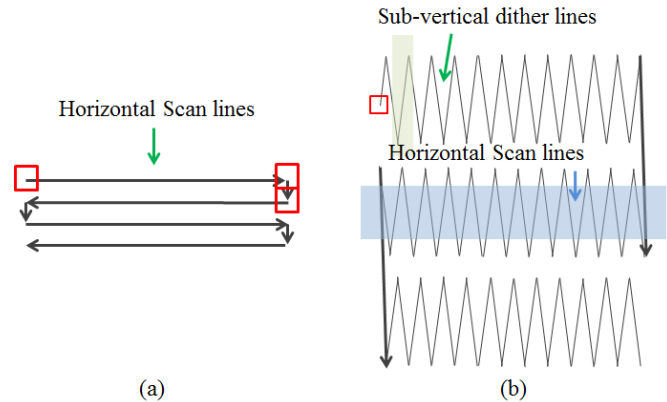

(a)   (b)

Figure 2. Illustration of the sub-vertical scanning. (a) the galvonometer scan pattern; (b) the dither scan pattern with the auxiliary scanner.

On the other hand, a 10mm × 10mm mirror can achieve 4 kHz scanning speed for ±10° optically scanning (= ±5° mechanical rotation). A commercial resonant scanner (EOPC, SC30-10X10) supporting this specification has a scanning capability of C ~ 4.1 × 10⁷ mm² ·deg² ·lines/sec (= 20° × 2.64° × 8,000 line/sec × 10mm × 10mm × 0.99, where 0.99 (=cos 5°) is the factor of the effective aperture considering the mirror rotation. Note that a VGA hologram imaged on the 10mm × 10mm mirror has a viewing angle of 2.64°×1.98° for the 450nm wavelength. We use the 2.64° side as the $\Delta\theta_y$), which is 10 times higher than the previous scanner. However, it cannot be used to replace the first axis of the galvanometer due to the image size requirement. Also note that, for the resonant scanner set-up, the scanning direction is y axis, and the supported viewing angle is the horizontal scanning range in y axis

and $\Delta\theta_x$ in x axis for each scan line. It is a bit different to what has been described previously, but it is of the same concept of using the supported viewing angle of each scan line.

We conclude that a scanner with a smaller mirror with a higher scan frequency has a higher information distribution capability than the galvanometer with a smaller mirror and a higher scan frequency.

We realized that a rapidly driven scanner, such as a resonant scanner, with a smaller mirror can be used as an auxiliary third scanner to augment the existing galvanometer to improve the previous system's scanning capability. Images can be delivered to the mirror of the resonant scanner, which is rapidly scanning, and then imaged onto the mirror of the galvanometer. The scanning direction of the resonant scanner is perpendicular to the first axis of the galvanometer, and the second axis of the galvanometer applies a step wider than its original step. This effectively introduces sub-vertical dithered scan lines into the original scan line patterns, as shown in the right part of Fig.2. Fig.3 illustrates the CIH system integrated with a resonant scanner.
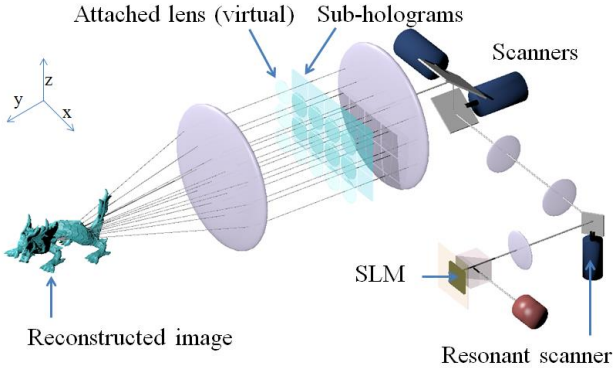

Figure 3. Illustration of the CIH system integrated with a resonant scanner. Note that it is just an illustration and it is not to the actual scale.

We use a resonant scanner (EOPC, SC30-10X10) supporting 10mm × 10mm mirror and 4 kHz scanning speed for ±10° optically scanning as our auxiliary third scanner to prove the concept. Since the first axis of the CIH system is scanning at 140 scanlines/sec, the 4 kHz scanning rate of the third scanner can provide more than 50 sub-vertical dither lines for each horizontal scanline. In our use, we use 45-degree reflection, as shown in Fig.3, and the factor of effective aperture becomes 0.64 (= cos 50°). Besides we use 633 nm laser (red) as the light source for this proof-of-concept experiment. Each sub-vertical dither line provides space to accommodate additional sub-holograms in the vertical direction. Although, 50 sub-vertical dither lines is more than the number of sub-views in the first axis of the galvanometer (it has only 30 sub-views capacity), the additional sub-holograms in the height of the sub-vertical dither line means it can expand the system's overall vertical viewing angle. Each sub-vertical dither line can accommodate at most 10 sub-holograms. This number is calculated by the optical scanning range of the third scanner divided by the

viewing angle of the sub-hologram from the 10mm × 10mm mirror: 20°/1.98° ~ 10 (1.98° is the $\Delta\theta_x$ as mentioned earlier). This means we can expand the vertical angle up to 10 times, as well as the overall bandwidth of the opto-mechanical system.

To support numbers and calculations above, here are parameters used in our experiment. The SLM in use is a DMD with a resolution of 1,024 × 768 and a pixel pitch of 13.68 μm. The wavelength of the laser in use is 633 nm. We place a lens with a focal length of 200 mm in front of the SLM by 200 mm to reconstruct the Fourier hologram from the SLM onto the resonant scanner, which is placed another 200 mm away from the lens. The reconstructed image has a size of 9.3 mm × 9.3 mm (image size ~ f·λ/pitch). Since the DMD is a binary device, we only use half of the reconstructed image to avoid the conjugation image, and the effective image size is 4.7 mm × 9.3 mm, which is covered by the effective aperture. The 1,024 side of the SLM is parallel to the x axis in Fig.3, and it makes the viewing angle of the 4.7 mm × 9.3 mm reconstructed image 1.99°×1.50° (9.3 mm /1024 = 9.08 um, which is the equivalent imaged pitch on the mirror, and $\sin^{-1}$ 0.633/(2·9.08) = 1.99°; 9.3 mm /768 = 12.11 um, which is the equivalent imaged pitch on the mirror, and $\sin^{-1}$ 0.633/(2·12.11) = 1.50°). And then a 2.5× imaging system is placed after the SLM to project the image on the galvanometer mirror (by using a 100mm lens and a 250mm lens). Another imaging system with magnification of 2× is used (by using a 200mm lens and a 400mm lens) after the galvanometer to further enlarge the image.

The auxiliary third scanner we use for the proof-of-concept uses a closed-loop control, which doesn't allow it to be synchronized with other devices. Therefore, in our test, images are the same for each sub-vertical scan line, but still change along the horizontal scanning and vertical scan line. Since the resonant scanner is not synchronized with other devices, there is no need to apply pulsed laser, and a continuous laser is in use, thereby the reconstruction result shows a bit blurring as mentioned earlier. The result is provided in the result video [12], which shows that the overall vertical viewing angle is enlarged. Each horizontal scanline (between the vertical viewing gap jumps we introduced intentionally) has more than 2° viewing angle.

Note that a sychronizable resonant scanner is not available on the market, to our best knowledge. Customizing such a device can even better demonstrate the proposed approach, and is regarded as a future work.

A tenfold improvement in scanning capacity is promising. It then becomes the case that the DMD does not match up with the scanning capacity, and is now the limiting factor. This allows us to use the DMD with higher bandwidth or even to integrate multiple DMDs into the system. For example, the current architecture uses one DMD to sequentially provide R/G/B colors. With the 10 times improvement in scanning capacity, we can use three DMDs, each of them is in charge of one color channel. Assuming we can use the full 22,727 Hz frame

rate of three VGA DMDs, it will be able to provide 53.6 Gbits/sec of bandwidth in a single system.

In conclusion, we introduced the use of an auxiliary resonant scanner in a previously proposed scanned CIH system to implement the sub-vertical dither scanning. This proposed system can accommodate the frame rate of a VGA DMD up to around 126k frames/sec rate, which is possible to be achieved in the future. By taking the advantage of the high scanning ability of a resonant scanner, the overall visual extent, in terms of viewing angle and image size, can be expanded by multiple times.

Reference

1. B. L. Anderson and K. Nakayama, "Toward a general theory of stereopsis: Binocular matching, occluding contours, and fusion" Psychol. Rev. 101(3), 1994, pp.414–445.

2. V. Bruce, P. R. Green, and M. A. Georgeson, Visual Perception: Physiology, Psychology, & Ecology, Psychology Press, 2003.

3. F. Yaraş, K. Hoonjong and L. Onural. "State of the art in holographic displays: a survey." Journal of display technology 6.10, 2010, pp. 443-454.

4. V.M. Bove, "Display holography's digital second act." Proceedings of the IEEE 100.4, 2012, pp. 918-928.

5. J. E. Greivenkamp, Field Guide to Geometrical Optics, SPIE PRESS, 2004, pp.28.

6. J. S. Chen, Q. Y. J. Smithwick and D. P. Chu. "Coarse integral holography approach for real 3D color video displays." Optics express 24.6, 2016, pp. 6705-6718.

7. J. S. Chen and D. P. Chu."Improved layer-based method for rapid hologram generation and real-time interactive holographic display applications." Optics Express 23.14, 2015, pp. 18143-18155.

8. H. Kakeya, T.Kurokawa and Y. Mano, "Electronic realization of coarse integral volumetric imaging with wide viewing angle.", Proc. SPIE. 7524, 2010, pp.752411.

9. H. Kakeya, "Formulation of coarse integral imaging and its applications.", Electronic Imaging. International Society for Optics and Photonics, 2008, pp.680317.

10. Y. Takaki and N. Okada, "Hologram generation by horizontal scanning of a high-speed spatial light modulator," Appl. Opt. 48, 2009, pp.3255-3260.

11. Z.M.A. Lum, X. Liang, Y. Pan, R. Zheng and X. Xu, "Increasing pixel count of holograms for three-dimensional holographic display by optical scan-tiling", Optics Engineering, 52(1), 2013, pp.015805.

12. [video link]

13. Stanford Computer Graphics Laboratory, https://graphics.stanford.edu/data/3Dscanrep/

14. D.Y. Chen, X.P. Tian, Y.T. Shen and M. Ouhyoung, "On Visual Similarity Based 3D Model Retrieval", Computer Graphics Forum (EUROGRAPHICS'03), 22(3), 2003, pp.223-232.

15. NTU 3D Model database, http://3d.csie.ntu.edu.tw/~dynamic/database/